



Extreme dust storm over the eastern Mediterranean in September 2015: Lidar vertical profiling of desert dust at Limassol, Cyprus

Rodanthi-Elisavet Mamouri^{1,2}, Argyro Nisantzi¹, Albert Ansmann³, and Diofantos G. Hadjimitsis¹

¹Cyprus University of Technology, Department of Civil Engineering and Geomatics, Limassol, Cyprus

²National Observatory of Athens, Athens, Greece

³Leibniz Institute for Tropospheric Research, Leipzig, Germany

Correspondence to: R.-E. Mamouri (rodanthi.mamouri@cut.ac.cy)

Abstract. An unusually strong dust outbreak towards Cyprus occurred in September 2015. Mass concentrations exceeding 10000 $\mu\text{g}/\text{m}^3$ were estimated from visibility studies at Limassol (visibilities around 500m on 8 September). Surprisingly, dust transport models failed to predict this record dust event. We present MODIS products (aerosol optical thickness AOT), surface PM_{10} observations, visibility studies, and lidar profiling results (covering the main dust period from 7-11 September 2015). Vertical aerosol layering was dominated by a two-layer structure with layers from the ground to 1500 m and from about 1500-3500 m height. The maximum dust AOT reached probably values between 6-10 and was higher than 1 over Cyprus for more than three days. Dust particle extinction coefficients (532 nm) and mass concentrations up to 1300 Mm^{-1} and 2700 $\mu\text{g}/\text{m}^3$, respectively, were observed with lidar in the elevated layers on 7 September, when first dense dust plumes crossed the EARLINET lidar station at Limassol. Raman lidar retrievals yield typical Middle East dust lidar ratios of 35-45 sr at 532 nm. The 532 nm particle linear depolarization ratio assumed values around 0.3.

1 Introduction

On 8 September 2015, a severe desert dust storm hit Cyprus. The visibility decreased to about 500 m, correspondingly the volume extinction coefficient of particles increased from clear sky values of 50-100 Mm^{-1} to 4500-6000 Mm^{-1} at 500 nm wavelength and the dust mass concentration most likely exceeded 10000 $\mu\text{g}/\text{m}^3$. The Air Quality Department (Department of Labour Inspection of Cyprus) published record PM_{10} dust mass concentrations of up to 7600 $\mu\text{g}/\text{m}^3$ at Limassol. PM_{10} denotes the mass concentration of particles with aerodynamic diameter smaller than 10 μm . Surprisingly, this extremely strong dust outbreak from deserts in northern Syria and Irak was not predicted by state-of-the-art dust transport models.

In this article, we summarize our lidar observation of this severe dust event. Goal is to provide a vertically resolved view on this unique dust episode and to compile complementary optical and microphysical particle information from in situ, lidar, and satellite observations which may be helpful for the modeling community when re-analyze the atmospheric meteorological conditions over the potential dust source regions to identify the reasons for the failure of the dust models to forecast this dust storm.

After a short description of the lidar and data analysis methods in Sect. 2, we present our observations in Sect 3. MODIS imaginary is used to describe the dust distribution in terms of dust optical thickness in the Cyprus region and the eastern



Mediterranean (Sect. 3.1). According to photographs taken from a high building in the center of Limassol, the horizontal visibility could be accurately determined during the maximum dust load on 8 September 2015 and the corresponding maximum dust particle extinction coefficient and the related dust mass concentration at 50 m above sea level (a.s.l.) could therefore be estimated with good accuracy (Sect. 3.2). In situ observations of particle mass concentration at six sites in Cyprus are discussed in Sect. 3.2 as well. The lidar observation from 7-11 September 2015 are then presented in terms of height-time displays of aerosol layering and dust layer evolution (Sect. 3.3) and height profiles of particle backscatter, extinction, lidar ratio, linear depolarization ratio (Sects. 3.4), and mass concentration profiles (Sect. 3.5). Concluding remarks are given in Sect. 4.

2 Instrumentation

The lidar station of the Cyprus University of Technology (CUT) at Limassol is equipped with a 532 nm polarization/Raman lidar (with an additional channel at 1064 nm) and measures nitrogen Raman signal profiles at 607 nm. The lidar station belongs to the European Aerosol Research Lidar Network EARLINET (Pappalardo et al., 2014). The CUT lidar instrument is described by Mamouri et al. (2013), Mamouri and Ansmann (2014), and Nisantzi et al. (2014, 2015). Details of the complex data analysis are given by Mamouri et al. (2012, 2013) and Mamouri and Ansmann (2014, 2015). The EARLINET lidar is collocated with an AERONET photometer (Holben et al., 1998; Nisantzi et al., 2015). Unfortunately, the CUT-TEPAK AERONET photometer was not available from July to October 2015 for calibration reasons.

3 Results

3.1 MODIS satellite observations

We used satellite imagery (Moderate Resolution Imaging Spectroradiometer, MODIS, <http://lance-modis.eosdis.nasa.gov/>) to obtain an overview of the dust storm in terms of aerosol optical thickness (AOT). As can be seen in Fig. 1, optically dense dust plumes were advected from the east and reached Cyprus on 7 September 2015. The dust plumes were partly so dense that the dark surface of the Mediterranean Sea and parts of the island of Cyprus, especially southern Cyprus, were no longer visible from space. The highest dust load was observed over Cyprus on 8 September 2015. The dust amount slowly decreased on 10–11 September, and more rapidly on 12–13 September. The Troodos mountains (dark area in central western Cyprus) with top heights up to 2000 m were always visible during the dust storm. This indicates that the thickest dust layers crossed Cyprus at heights below 1500 m height.

Figure 2 shows time series of AOT retrieved from daily MODIS observations for five coastal sites from Risocarpaso at the most eastern tip of Cyprus to Pafos, which is approximately 250 km southwest of Risocarpaso. In addition, the AOT time series for the capital city Nicosia is shown. The maximum and mean AOT values for areas with radius of 50 km around these cities are presented. Note, that the maximum AOT, retrievable from the MODIS data, is 5 so that many of the values on 8 September (Julian day 251) are biased. Our observations in Sects. 3.2–3.4 suggest peak AOT values over Cyprus of 6–10. For



the comparison with our lidar observations the stations of Larnaca and Limassol are most relevant. One can see that the AOT was around and above 1.0 for more than three days.

3.2 Surface in situ PM₁₀ observations and dust load estimates from visibility studies

Figure 3 shows four photographs taken from the roof of a high building (AERONET station) at Limassol to the south and north. The left photographs show the situation during the phase with the heaviest dust load (8 September, around local noon). These pictures are in strong contrast to the photographs taken one day later, when the dust concentration was still high but the horizontal visibility increased already to values of around 20 km. By careful inspection of the pictures from 8 September (searching for different pronounced buildings and towers) we estimated the horizontal visibility, i.e., the meteorological optical range (MOR) and determined values around 500 m, but clearly below 750 m. Our estimation is in good agreement with observations from pilots (during landing at the International Airport of Larnaca) who also reported horizontal visibilities of 500 m on 8 September 2015.

MOR (after the definition of the World Meteorological Organization) is related to the intuitive concept of visibility through the contrast threshold and this threshold is taken as 0.05. It is assumed that, when an observer can just see and recognize a dark object against the bright horizon, the apparent contrast of the object is 0.05. The atmospheric transmission (close to 1.0 for rather clear skies) is reduced to 0.05 when the AOT is 3.0 (at wavelengths around 550 nm). This means that the mean particle extinction coefficient along a horizontal path must be 6000 Mm⁻¹ (or 4500 Mm⁻¹) in the case of MOR of 500 m (or 750 m). By using a typical dust extinction-to-mass conversions factor of 2 μg/m³/Mm⁻¹ (Ansmann et al., 2012), these very high dust extinction coefficients point to dust mass concentrations of 9000-12000 μg/m³.

Figure 4 presents surface observations of PM₁₀ concentrations from 6-14 September 2015. Hourly mean values for six sites across Cyprus are shown. These PM₁₀ observations were performed by the Air Quality Department (Department of Labour Inspection) of Cyprus at Limassol and are available at <http://www.airquality.dli.mlsi.gov.cy/>. The data were directly downloaded, are not validated, and thus may contain errors. As can be seen, maximum dust mass concentrations at Limassol were close to 8000 μg/m³ on 8 September. Our higher estimates of 9000-12000 μg/m³ can be explained by the fact that PM₁₀ measurements only cover the particle size range up to particle diameters of 10 μm. Larger particles, obviously present during this extraordinary dust storm, can not pass the PM₁₀ inlet of the aerosol measuring system so that the total mass concentration is underestimated at these conditions.

3.3 Lidar overview: vertical dust layering

Figure 5 provides an overview of the lidar observations at Limassol from 7-11 September 2015. Two pronounced dust layers were observed during the early stage of the dust storm in the evening of 7 September 2015. First thick dust layers crossed Cyprus at heights between 2 and 3.7 km. A two-layer structure established and probably prevailed on 8 September, the day with the highest dust load. The rather thick dust layer obviously reached to 1000-1500 m height on 8 September, in agreement with the MODIS observations in Fig. 1. The higher parts of the Troodos mountains (dark area) above 1000 m height remained



always visible in Fig. 1, even on 8 September, while the southern parts of Cyprus (Limassol and Larnaca area) were totally covered by dense dust layers so that the surface was no longer visible in the satellite images on 8 September.

Unfortunately, lidar observations were not possible on 8 September because of the rather high dust particle concentration. No attempt was made to run the lidar to avoid any possible damage of the lidar optics and sensitive light detection units.

5 However, if we assume a surface near homogeneous dust layer up to 1000-1500 m with particle extinction coefficients of 4500-6000 Mm^{-1} , as our visibility observations indicate, and a second, less dense dust layer on top with an AOT close to 1, we end up with a total dust AOT in the range of 6-10 on 8 September 2015.

On 9 September 2015 (15:00-21:30 UTC), the general two-layer structure as observed on 7 September was still present. The strongest lidar signals (red layer on 9 September in Fig. 5) were measured in a shallow layer close to the ground, below about
10 500–800 m height. These strong lidar signals on 9 September as well as on 11 September are in accordance with the high dust PM_{10} values measured in situ on these days (see Fig. 4).

On 10–11 September 2015, two lidar measurement sessions were conducted, one during morning and noon hours (6:20–14:20 UTC) and one during the evening (from about 17:00–21:25 UTC). Heterogeneous structures, temporally as well as vertically, still prevailed on 10 September (morning/noon session). In the evening of 10 September, again an elevated optically
15 dense dust layer crossed the EARLINET lidar station. Top heights decreased to below 3000 m. On 11 September, a more homogeneous and temporally constant layering was found. The main layer was now below 2000 m. Traces of dust were detected still up to 3000–4000 m height.

The observed dust layering with layers mainly below 3000 m height can be regarded as typical for Middle East dust outbreaks (Nisantzi et al., 2015). In contrast, Saharan dust plumes frequently reach 5-8 km height over Cyprus. Such an observation is
20 presented by Mamouri and Ansmann (2015).

3.4 Lidar-derived profiles of dust optical properties

In Fig. 6, we present profiles of particle backscatter and extinction coefficients at 532 nm, the corresponding extinction-to-backscatter ratio (lidar ratio), and the particle linear depolarization ratio at 532 nm for each of the four evenings on 7 and 9–11 September. 1-hour to 3-hour mean profiles provide an overview of the main features of the dust layers in terms of dust optical
25 properties. The backscatter coefficients are obtained with high vertical resolution (signal smoothing window length of 195 m) and show best the layer structures.

The extinction coefficients and corresponding lidar ratios are calculated from smoothed Raman signal profiles (nitrogen Raman backscatter at 607 nm wavelength, 375m smoothing length). The particle extinction coefficients reached values of 1300 Mm^{-1} in the lower layer and were around 350 Mm^{-1} in the second layer on 7 September. Another dust front caused
30 extinction coefficients up to 550 Mm^{-1} in an elevated layer between 1000 and 2500 m height on 10 September 2015.

The lidar ratios at 532 nm were 35-45 sr in the dust layers on 7 September, 45-60 sr on 9 September, 40-45 sr on 10 September, and 50-60 sr on 11 September. Values of 35-45 sr are typical for desert dust from Middle East dust sources (Mamouri et al., 2013; Nisantzi et al., 2015). Larger lidar ratios on 9 and 11 September indicate a mixture of dust and anthropogenic haze.



The particle linear depolarization ratio assumed typical dust values around 0.3 (7 and 10 September) in the dense dust layers. These values clearly indicate the dominance of desert dust above Limassol on these days. The decrease towards values of 0.21-0.26 on 9 and 11 September reflects the increasing impact of anthropogenic haze on the optical properties of the advected air masses.

5 3.5 Lidar-derived dust mass concentrations

Figure 7 finally shows the estimated profiles of dust mass concentrations, observed in the evenings of 7, 9, 10, and 11 September 2015. The technique applied to derive dust mass concentrations from the profiles of the particle backscatter coefficient and linear depolarization ratio in Fig. 6 is described by Ansmann et al. (2011); Ansmann et al. (2012), and Mamouri and Ansmann (2014). The values exceeded $2500 \mu\text{g}/\text{m}^3$ below 1500 m height and $750 \mu\text{g}/\text{m}^3$ around 3 km height on 7 September 2015, before the extreme dust front crossed Cyprus on 8 September. During the passage of the dust front on 10 September, the dust mass concentrations were again close to $1200 \mu\text{g}/\text{m}^3$ in the center of the elevated layer from 1000-2500 m height. Even mass concentrations of $200\text{-}300 \mu\text{g}/\text{m}^3$ as observed on 9 and 11 September 2015 are clearly above the threshold value for a significant dust event (defined by the occurrence of mass concentrations $>100 \mu\text{g}/\text{m}^3$).

3.6 HYSPLIT backward trajectories

We briefly discuss the backward trajectories for this extreme dust event. The HYSPLIT (HYbrid Single-Particle Lagrangian Integrated Trajectory, <http://www.arl.noaa.gov/HYSPLIT.php>) model was used for this purpose (Stein et al., 2015). As mentioned, dust transport models failed to predict this dust episode. Figure 8 shows backward trajectories for 8 September 2015 (9 UTC) for arrival heights over Limassol (33°E) and about 160 km east of Limassol (35°E). The backward trajectories for Limassol are in strong contradiction with our dust observations. Only the trajectories for 35°E indicate dust advection from northern Syria and Iraq. However, the predicted dust mass loads for 35°E were too low. According to Fig. 1, which indicates similar conditions 160 km east of Cyprus and over Cyprus on 8 September, the mass concentration was underestimated by more than 2 orders of magnitude. The erroneous dust predictions for the Cyprus region is related to the meteorological fields (temperature and wind fields) which did not allow dust transport further to the west than 35° , and probably also to not well-known meteorological conditions in the dust source regions which lead to a strong underestimation of dust mobilization as will be discussed in a follow-up paper.

4 Conclusions

A unique dust outbreak has been discussed. The extreme dust storm was documented by means of satellite, lidar, and surface in situ observations. Dust AOT values of the order of 6-10 occurred over Cyprus on 8 September 2015. Maximum dust particle mass concentrations at Limassol were of the order of $10000 \mu\text{g}/\text{m}^3$ as estimated from visibility observations. The vertical dust layering and the optical and microphysical characteristics of the observed desert dust layers were discussed on the basis of Limassol lidar observations. Dust mass concentrations of $750\text{-}2700 \mu\text{g}/\text{m}^3$ were derived from the lidar observations above



1000 m height on 7 and 10 September 2015, when lidar observations were possible. Typical Middle East dust lidar ratios of 35-45 sr were measured with the Raman lidar.

Acknowledgements. The authors thank ERATOASTHENES Research Center for their support. R.-E. M. would like to thank CUT's library for the financial support within Cyprus University of Technology Open Access Author Fund. The authors acknowledge support through
5 the following projects and research programs: ACTRIS Research Infrastructure (EU H2020-RI) under grant agreement no. 654169, BEYOND (Building Capacity for a Centre of Excellence for EO-based monitoring of Natural Disasters, FP7-REGPOT-2012-2013-1) under grant agreement no. 316 210, BACCHUS (impact of Biogenic vs. Anthropogenic emissions on Clouds and Climate: towards a Holistic UnderStanding, EU FP7-ENV-2013) under grant agreement project number 603445, and GEO-CRADLE (EU H2020 R&I) under grant agreement No 690133. The authors are very thankful to the Air Quality Department (Department of Labour Inspection) for establishing and
10 maintaining the air quality stations of Republic of Cyprus. The authors gratefully acknowledge the NOAA Air Resources Laboratory (ARL) for the provision of the HYSPLIT transport and dispersion model as well for the provision of Global Data Assimilation System (GDAS) data used in this publication. The Terra/MODIS Aerosol Daily datasets were acquired from the Level-1 Atmosphere Archive and Distribution System (LAADS) Distributed Active Archive Center (DAAC), located in the Goddard Space Flight Center in Greenbelt, Maryland (<https://ladsweb.nascom.nasa.gov/>). We acknowledge the use of data products or imagery from the Land, Atmosphere Near real-time Capa-
15 bility for EOS (LANCE) system operated by the NASA/GSFC/Earth Science Data and Information System (ESDIS) with funding provided by NASA/HQ.



References

- Ansmann, A., Tesche, M., Seifert, P., Groß, S., Freudenthaler, V., Apituley, A., Wilson, K. M., Serikov, I., Linné, H., Heinold, B., Hiebsch, A., Schnell, F., Schmidt, J., Mattis, I., Wandinger, U., and Wiegner, M.: Ash and fine-mode particle mass profiles from EARLINET-AERONET observations over central Europe after the eruptions of the Eyjafjallajökull volcano in 2010, *J. Geophys. Res.*, 116, D00U02, doi:10.1029/2010JD015567, 2011.
- 5 Ansmann, A., Seifert, P., Tesche, M., and Wandinger, U.: Profiling of fine and coarse particle mass: case studies of Saharan dust and Eyjafjallajökull/Grimsvötn volcanic plumes, *Atmos. Chem. Phys.*, 12, 9399–9415, doi:10.5194/acp-12-9399-2012, 2012.
- Holben, B. N., Eck, T. F., Slutsker, I., Tanré, D., Buis, J. P., Setzer, A., Vermote, E., Reagan, J. A., Kaufman, Y. J., Nakajima, T., Lavenu, F., Jankowiak, I., and Smirnov, A.: AERONET – A federated instrument network and data archive for aerosol characterization, *Remote Sens. Environ.*, 66, 1–16, 1998.
- 10 Mamouri, R. E., Papayannis, A., Amiridis, V., Müller, D., Kokkalis, P., Rapsomanikis, S., Karageorgos, E. T., Tsaknakis, G., Nenes, A., Kazadzis, S., and Remoundaki, E.: Multi-wavelength Raman lidar, sun photometric and aircraft measurements in combination with inversion models for the estimation of the aerosol optical and physico-chemical properties over Athens, Greece, *Atmos. Meas. Tech.*, 5, 1793–1808, doi:10.5194/amt-5-1793-2012, 2012.
- 15 Mamouri, R. E., Ansmann, A., Nisantzi, A., Kokkalis, P., Schwarz, A., and Hadjimitsis, D.: Low Arabian dust extinction-to-backscatter ratio, *Geophys. Res. Lett.*, 40, 4762–4766, doi:10.1002/grl.50898, 2013.
- Mamouri, R. E. and Ansmann, A.: Fine and coarse dust separation with polarization lidar, *Atmos. Meas. Tech.*, 7, 3717–3735, doi:10.5194/amt-7-3717-2014, 2014.
- Mamouri, R. E. and Ansmann, A.: Estimated desert-dust ice nuclei profiles from polarization lidar: methodology and case studies, *Atmos. Chem. Phys.*, 15, 3463–3477, doi:10.5194/acp-15-3463-2015, 2015.
- 20 Nisantzi, A., Mamouri, R. E., Ansmann, A., and Hadjimitsis, D.: Injection of mineral dust into the free troposphere during fire events observed with polarization lidar at Limassol, Cyprus, *Atmos. Chem. Phys.*, 14, 12155–12165, doi:10.5194/acp-14-12155-2014, 2014.
- Nisantzi, A., Mamouri, R. E., Ansmann, A., Schuster, G. L., and Hadjimitsis, D. G.: Middle East versus Saharan dust extinction-to-backscatter ratios, *Atmos. Chem. Phys.*, 15, 7071–7084, doi:10.5194/acp-15-7071-2015, 2015.
- 25 Pappalardo, G., Amodeo, A., Apituley, A., Comeron, A., Freudenthaler, V., Linné, H., Ansmann, A., Bösenberg, J., D’Amico, G., Mattis, I., Mona, L., Wandinger, U., Amiridis, V., Alados-Arboledas, L., Nicolae, D., and Wiegner, M.: EARLINET: towards an advanced sustainable European aerosol lidar network, *Atmos. Meas. Tech.*, 7, 2389–2409, doi:10.5194/amt-7-2389-2014, 2014.
- Stein, A. F., Draxler, R. R., Rolph, G. D., Stunder, B. J. B., Cohen, M. D., and Ngan, F.: NOAA’s HYSPLIT Atmospheric Transport and Dispersion Modeling System. *Bull. Amer. Meteorol. Soc.*, 96, 2059–2077, doi: 10.1175/BAMS-D-14-00110.1, 2015

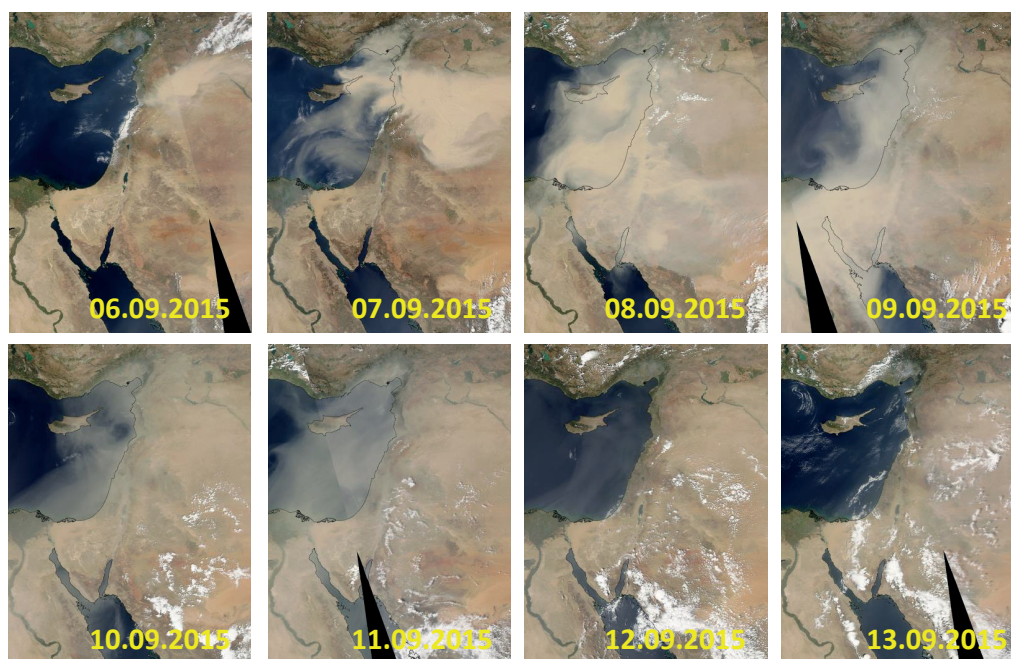


Figure 1. Dust outbreak towards Cyprus in September 2015 as seen from space (AQUA-MODIS, 10:30-11:30 UTC overpasses, <http://lance-modis.eosdis.nasa.gov/>).

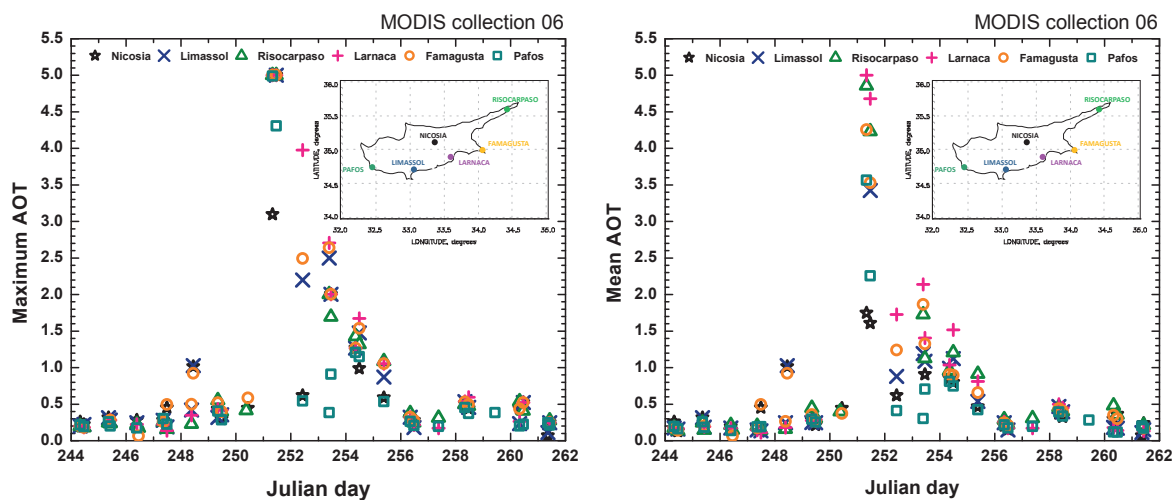


Figure 2. MODIS-derived maximum (left) and mean (right) 550 nm aerosol optical thickness (AOT) for six sites in Cyprus for the period from 1–18 September 2015. The maximum and mean AOTs are determined from all values within areas with 50 km radius around the six sites. The highest AOTs occurred on Julian day of 251 (8 September 2015). MODIS data are available at <http://ladsweb.nascom.nasa.gov/data/search.html>.

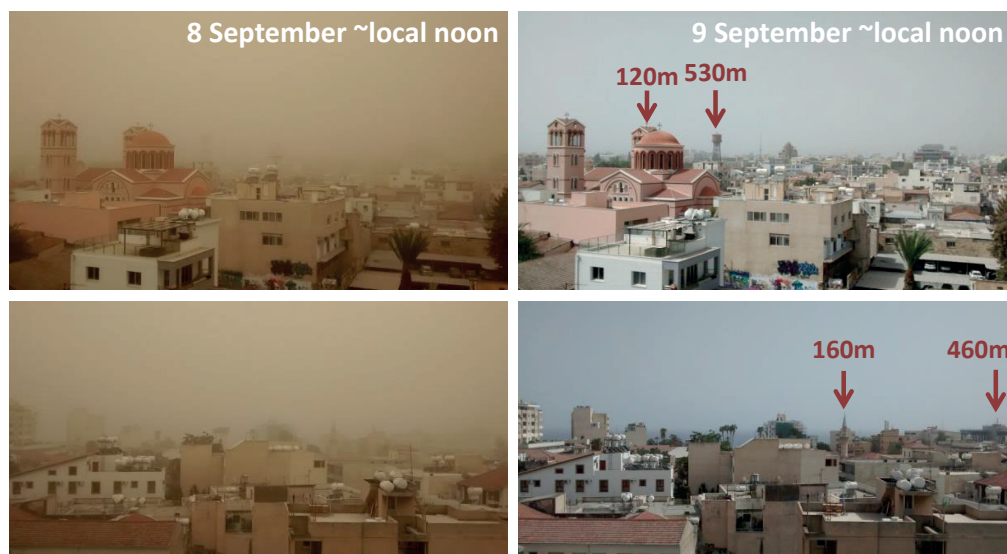


Figure 3. Photographs taken at the roof of a high building (CUT-TEPAK AERONET site) in the city center of Limassol to the north (top) and south (bottom) on 8 September 2015, 8:20–8:30 UTC (left) and on 9 September 2015 (right), again around local noon. The meteorological optical range (or horizontal visibility) was about 500 m on 8 September and higher than 20 km on 9 September 2015. Distances to several towers from the AERONET station are indicated.

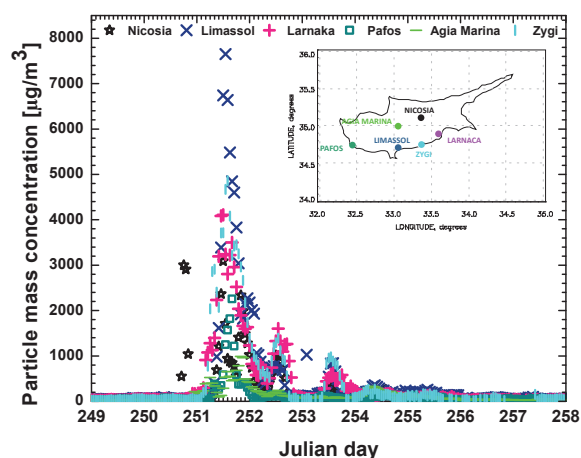


Figure 4. Hourly mean values of the PM_{10} particle mass concentrations measured at six locations in Cyprus. The in situ aerosol observations are performed by the Air Quality Department (Department of Labour Inspection of Cyprus at Limassol) and are available at <http://www.airquality.dli.mlsi.gov.cy/>. The peak PM_{10} concentration of $7600 \mu\text{g}/\text{m}^3$ was observed around 9 UTC on 8 September 2015 (Julian day 251)

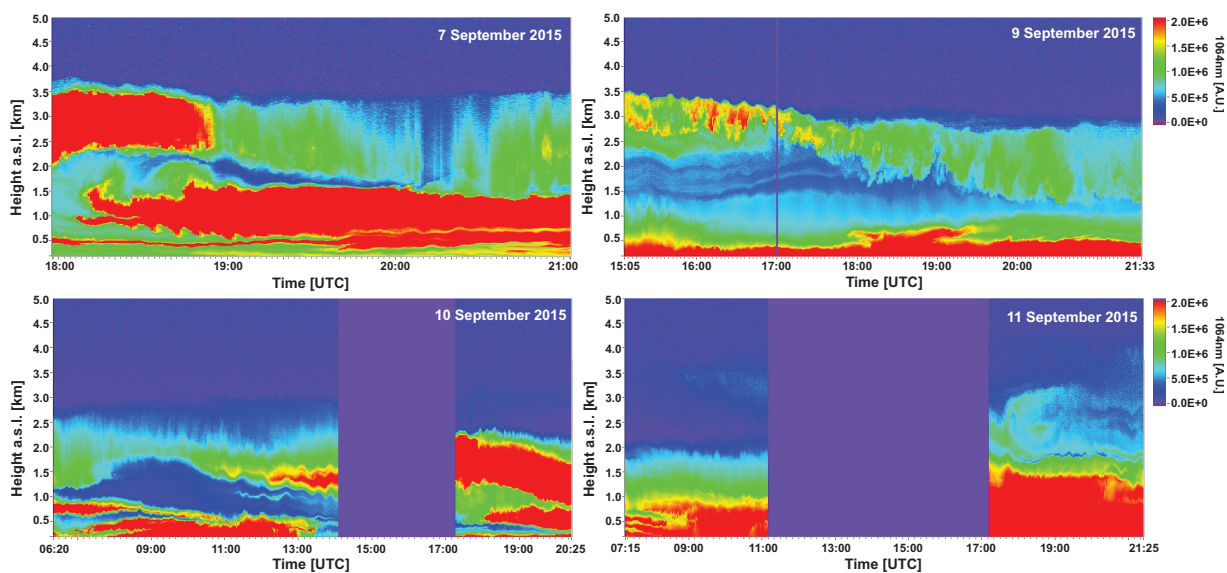


Figure 5. Desert dust layers observed with lidar over the EARLINET station of Limassol, Cyprus, on 7, 9, 10, and 11 September 2015. Range-corrected 1064 nm backscatter signals (in arbitrary units, A. U.) are shown. Red colors indicate rather dense dust plumes with particle extinction coefficients in the range of 500–1500 Mm^{-1} . The signals backscattered by dust in the elevated layers above 1000–1500 m height are partly strongly attenuated by the desert particles occurring below 1500 m. As a consequence, the elevated layers are mostly given in blue and green instead of red (as it would be the case after the correction of the attenuation effect).

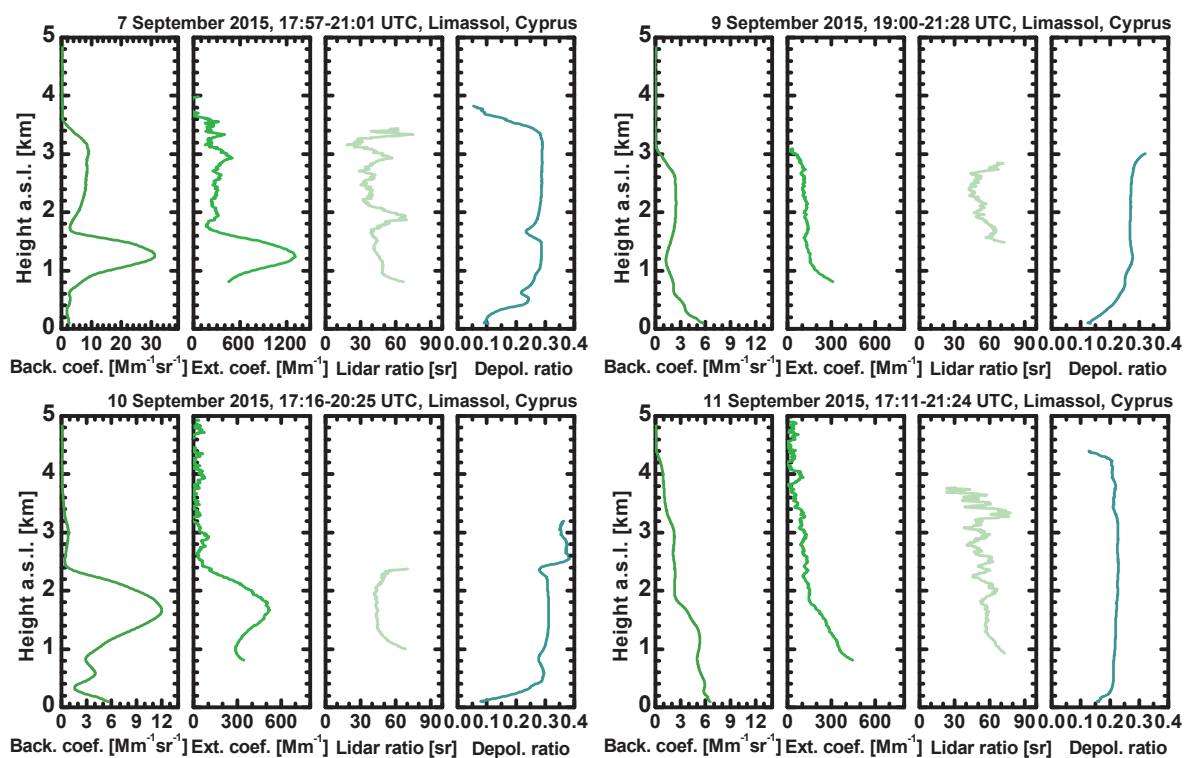


Figure 6. Mean vertical profiles of the 532 nm particle backscatter coefficient, extinction coefficient, lidar ratio, and particle linear depolarization ratio for the observational periods from 17:57–21:01 UTC on 7 September 2015, 19:00–21:28 UTC on 9 September 2015, 17:16–20:25 UTC on 10 September 2015, and 17:11–21:24 UTC on 11 September 2015. The Raman lidar method is applied. Vertical signal smoothing with a window length of 375 m is applied before computing the extinction coefficients and lidar ratios. The signal smoothing length is 195 m for the shown backscatter coefficient and depolarization ratio profiles. Retrieval uncertainties are of the order of 10% (backscatter coefficient, depolarization ratio), 25% (extinction coefficient), and 30% (lidar ratio).

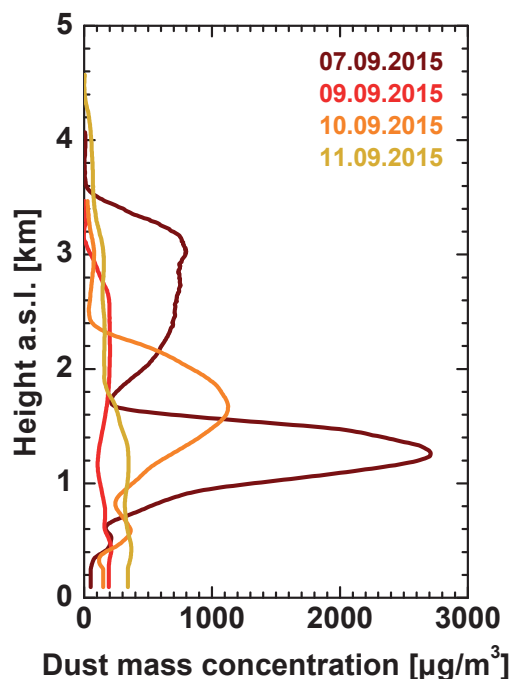


Figure 7. Dust mass concentration profiles derived from the lidar observations in Fig. 6. A dust particle mass density of 2.6 g/cm^3 is assumed in the retrieval. The overall uncertainty is 30% and mainly caused by the uncertainty in the dust volume-to-extinction ratio (extinction-to-volume conversion factor) assumed to be $0.8 \times 10^{-6} \text{ m}$.

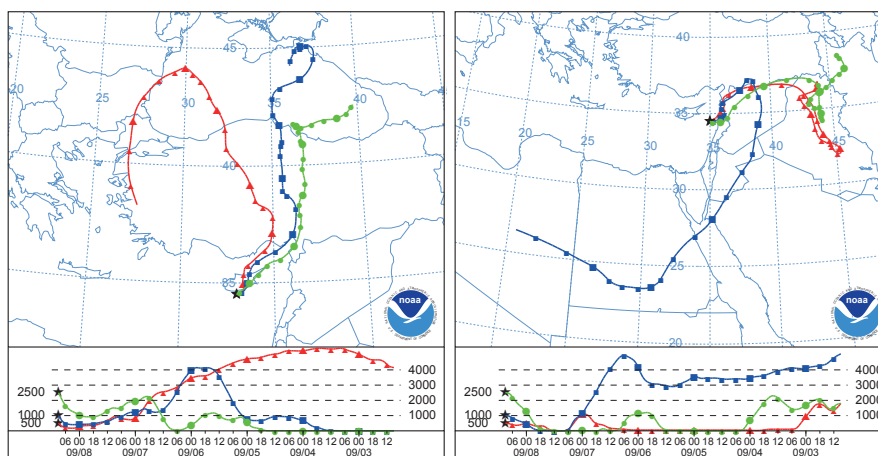


Figure 8. Six-day HYSPLIT backward trajectories (<http://www.arl.noaa.gov/HYSPLIT.php>) arriving at Limassol (33°E), Cyprus, at 500 m (red), 1000 m (blue), and 2500 m height (green) on 8 September 2015, 9 UTC (left), and at 35°E , about 160 km east of Limassol (right, arrival on 8 September, 9 UTC).